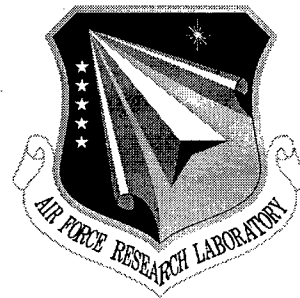


**AFRL-SN-RS-TR-1998-30**  
**Final Technical Report**  
**April 1998**



## **DUAL-MODE PHOTONIC DEVICES**

**Syracuse University**

**Joseph Chaiken**

*APPROVED FOR PUBLIC RELEASE; DISTRIBUTION UNLIMITED.*

19980603 054

**AIR FORCE RESEARCH LABORATORY**  
**SENSORS DIRECTORATE**  
**ROME RESEARCH SITE**  
**ROME, NEW YORK**

Although this report references limited documents (\*), listed on page 28, no limited information has been extracted.

This report has been reviewed by the Air Force Research Laboratory, Information Directorate, Public Affairs Office (IFOIPA) and is releasable to the National Technical Information Service (NTIS). At NTIS it will be releasable to the general public, including foreign nations.

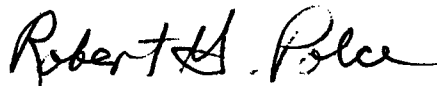
AFRL-SN-RS-TR-1998-30 has been reviewed and is approved for publication.

APPROVED:



REBECCA J. BUSSJAGER  
Project Engineer

FOR THE DIRECTOR:



ROBERT G. POLCE, Acting Chief  
Rome Operations Office  
Sensors Directorate

If your address has changed or if you wish to be removed from the Air Force Research Laboratory Rome Research Site mailing list, or if the addressee is no longer employed by your organization, please notify AFRL/SNDP, 25 Electronic Pky, Rome, NY 13441-4515. This will assist us in maintaining a current mailing list.

Do not return copies of this report unless contractual obligations or notices on a specific document require that it be returned.

<b>REPORT DOCUMENTATION PAGE</b>			Form Approved OMB No. 0704-0188	
Public reporting burden for this collection of information is estimated to average 1 hour per response, including the time for reviewing instructions, searching existing data sources, gathering and maintaining the data needed, and completing and reviewing the collection of information. Send comments regarding this burden estimate or any other aspect of this collection of information, including suggestions for reducing this burden, to Washington Headquarters Services, Directorate for Information Operations and Reports, 1215 Jefferson Davis Highway, Suite 1204, Arlington, VA 22202-4302, and to the Office of Management and Budget, Paperwork Reduction Project (0704-0188), Washington, DC 20503.				
1. AGENCY USE ONLY (Leave blank)		2. REPORT DATE April 1998	3. REPORT TYPE AND DATES COVERED FINAL Jun 96 - Jun 97	
4. TITLE AND SUBTITLE DUAL-MODE PHOTONIC DEVICES			5. FUNDING NUMBERS C - F30602-96-C-0171 PE - 62702F PR - 4600 TA - P5 WU - PM	
6. AUTHOR(S) Dr. Joseph Chaiken				
7. PERFORMING ORGANIZATION NAME(S) AND ADDRESS(ES) Syracuse University Department of Chemistry 113 Bowne Hall Syracuse NY 13244-1200			8. PERFORMING ORGANIZATION REPORT NUMBER  N/A	
9. SPONSORING / MONITORING AGENCY NAME(S) AND ADDRESS(ES) Air Force Research Laboratory/SNDP 25 Electronic Pky Rome NY 13441-4515			10. SPONSORING / MONITORING AGENCY REPORT NUMBER  AFRL-SN-RS-TR-1998-30	
11. SUPPLEMENTARY NOTES  Air Force Research Laboratory Project Engineer: Rebecca J. Bussjager, SNDP, x2918				
12a. DISTRIBUTION AVAILABILITY STATEMENT  APPROVED FOR PUBLIC RELEASE; DISTRIBUTION UNLIMITED			12b. DISTRIBUTION CODE	
13. ABSTRACT (Maximum 200 words) The goal of this effort was to exploit the physical interactions underlying the newly discovered photochromic optical memory system (POMS) in a different type of photonic device. The POMS approach had been used to implement optical control of optical data but now, because of the interrelated photochromism and electrochromism of the $WO_3 - W_2O_5$ system, hybrid devices can be envisioned. Such hybrid or "dual mode" devices would allow electrical control and manipulation of optical data, or conversely, optical control and manipulation of electronic domain data. POMS based devices could also allow simultaneous electronic or optical access to a single data set stored in a single location. Having the flexibility afforded by this family of devices will allow us to devise compound devices and eventually machines in which optical methods are used to their fullest advantage in interconnects and memory, and electronics are used to their fullest advantage in processing. This report explains experimental methods and discusses the results of a dual mode device.				
14. SUBJECT TERMS optical switch, nonlinear interface optical switches (NIOS) switch, photochromic dual mode device			15. NUMBER OF PAGES 40	
			16. PRICE CODE	
17. SECURITY CLASSIFICATION OF REPORT UNCLASSIFIED	18. SECURITY CLASSIFICATION OF THIS PAGE UNCLASSIFIED	19. SECURITY CLASSIFICATION OF ABSTRACT UNCLASSIFIED	20. LIMITATION OF ABSTRACT UNLIMITED	

## Introduction

The goal of this effort was to exploit the physical interactions underlying the newly discovered<sup>1,2,3</sup> photochromic optical memory system (POMS) in a different type of photonic device. The POMS approach had been used to implement optical control of optical data<sup>3</sup> but now, because of the interrelated photochromism and electrochromism of the  $\text{WO}_3$  -  $\text{W}_2\text{O}_5$  system, hybrid devices can be envisioned. Such hybrid or "dual-mode" devices would allow electrical control and manipulation of optical data, or conversely, optical control and manipulation of electronic domain data. POMS based devices could also allow simultaneous electronic or optical access to a single data set stored in a single location. We demonstrated this particular possibility earlier<sup>3</sup>. Having the flexibility afforded by this family of devices will allow us to devise compound devices and eventually machines in which optical methods are used to their fullest advantage in interconnects and memory, and electronics are used to their fullest advantage in processing.

Actually, the POMS process was discovered during an ES&E effort<sup>4</sup> titled "Optical Switch Evaluation" in which the goal was to evaluate nonlinear interface optical switches (NIOSs). In that effort, devices, i.e. switches, were fabricated using metal and metal oxide films deposited by laser chemistry of organometallics. These devices were to be fully optical in nature and applicable to a variety of Air Force needs related to computing, memory and interconnects. This effort: 1) revisits NIOS type devices armed with our recent development of the POMS concept, and 2) explores how to extend their optical operation into the electronic domain.

This final report will first review the basic ideas of NIOS operation and the electro and photochromism of the  $\text{WO}_3\text{-W}_2\text{O}_5$  system in the context of the POMS process. Then, experimental and procedural issues relating to device fabrication and evaluation will be presented. Finally, characterization and evaluation of all optical and “dual mode” NIOS devices will be presented. These results will show that “dual mode” and all optical NIOS device structures are in actual fact a very promising route to linking electronic and optical systems in new, novel and potentially useful ways.

### Nonlinear Interface Optical Switches

Tomlinson<sup>5</sup> proposed that it should be possible to produce all optical switching based on the following simple idea. It is known that there is a reflection whenever light traverses an interface between two media. The basic idea is to use materials whose indices of refraction can be equalized by appropriate stimulation. The reflection at the interface is switched. As illustrated in the diagram below, this effect can be accentuated using a prism in a configuration in which the light is incident on the interface at or near Brewster's Angle.

The switch, in this case, is comprised by the prism, having index of refraction  $n_1$ , the film, deposited on the hypotenuse of the prism having index of refraction  $n_2$ , and the surrounding air having index of refraction of 1. The film is the “active” part of the switch in that, under the influence

## Table of Contents

Introduction	1
Nonlinear Interface Optical Switches	2
The $\text{WO}_3\text{-W}_2\text{O}_5$ System	6
Experimental	12
Results	14
Discussion	25
Conclusion	28
References	28

### List of Figures

Figure 1	Simple all optical NIOS structure.	3
Figure 2a	Hybrid NIOS with external field.	4
Figure 2b	Electrocoloration type NIOS.	5
Figure 3	Representation of packing of $\text{WO}_6$ octahedra into lattice having either no edge-sharing octahedra, i.e. $\text{WO}_3(\text{top})$ , or having edge-sharing octahedra, $\text{WO}_{3-x}$ .	8
Figure 4	Optical set-up for probing prism type NIOS configurations.	15
Figure 5	Optical set-up for probing $\text{WO}_3$ films on planar substrates.	15
Figure 6	Angular response on three different positions on blue film.	17
Figure 7	Ramp experiment showing threshold for switching.	19
Figure 8	Oscilloscope trace showing two regimes of switching.	20
Figure 9	Appearance of "written" spots on blue film using red(top), white(middle), and blue(bottom) backlighting.	22
Figure 10	HeNe modulation as a function of applied 488 nm energy.	24

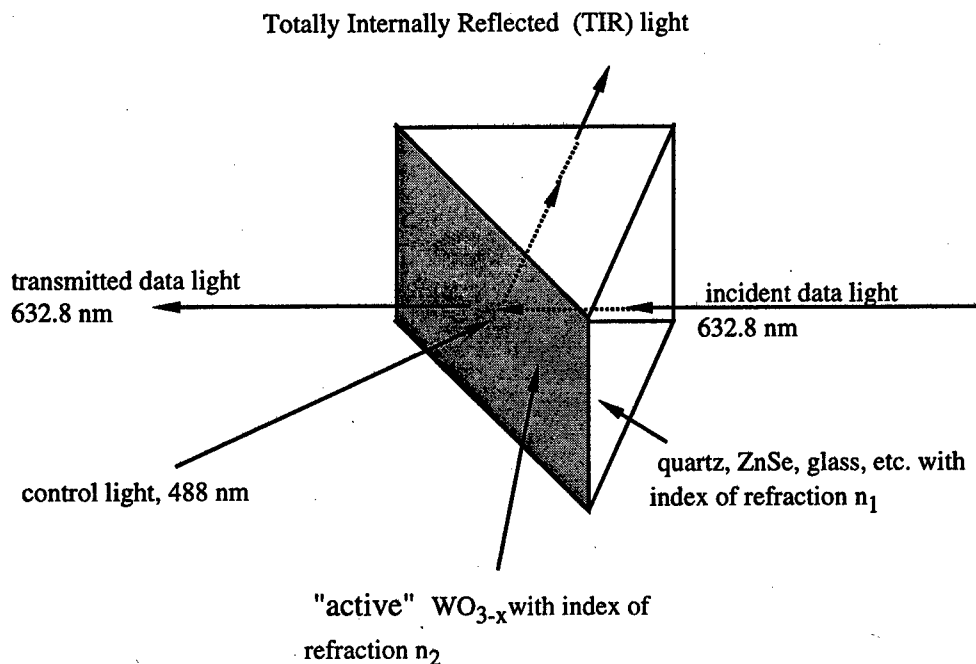


Figure 1. Simple all optical NIOS structure

of the "controlling" light, its index of refraction can change from  $n_2$  to  $n_2'$ . When this occurs, Brewster's Angle effectively changes and light can traverse the interface. Thus, the presence of the controlling light determines whether the data light traverses the interface and thereby turns the switch on or off.

This describes an all optical approach to NIOS design which we demonstrate in this report. In this particular idealized case, for example, there is no light traversing the interface unless there is an appropriate change in one or both of the indices of refraction of the two media involved. Using Brewster's angle maximizes the amplitude of the evanescent wave. This wave, as well as the direct interaction of any light



which does traverse the interface, provides energy to drive the switching. In fact, adapting work described by Crandall<sup>6</sup>, we performed tests on films configured as in Figure 2a and 2b. In the 2a version, we retain all the features of the purely optical version but also includes means

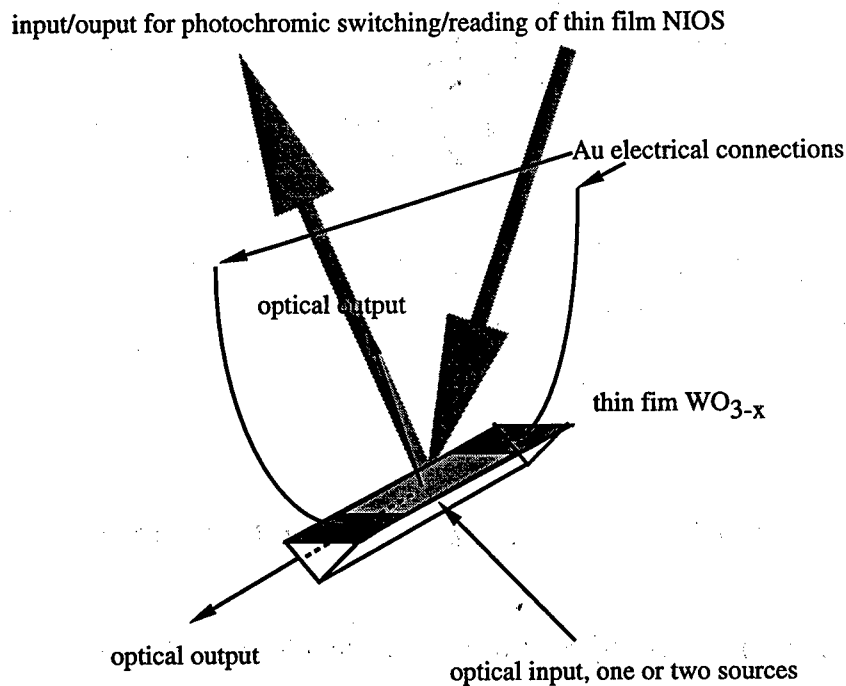


Figure 2a. Hybrid NIOS with external field

for applying an external, non-optical, electric field, parallel to the surface of the same film. A suitable material will be electrochromic such that upon application of the electric field, the index of refraction sensed by the input light will change and switching will again occur across the interface between the prism and the film.

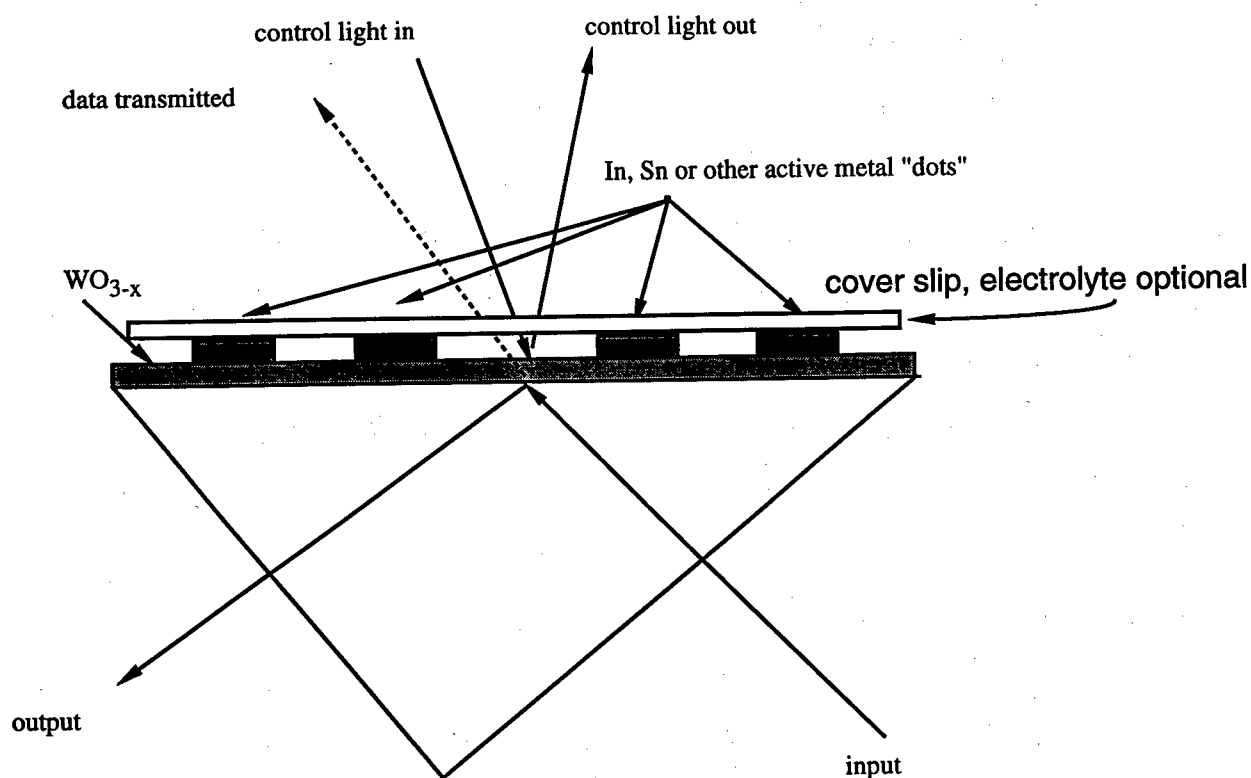


Figure 2b. Electrocoloration type NIOS

Of course, there are other ways of approaching the design of such a device, and each design involves many other details, but the above choices illustrate the basic idea. For example, electrochemical coloration, as shown in Figure 2b, does not necessarily require application of an electric field. However, many approaches employ a liquid electrolyte layer sandwiched between the prism and another solid phase, e.g. a metal coated cover slip. This does allow the applied electric field to be perpendicular to the film surface, but it also has the disadvantage of inducing spherical aberration into the light beams, which tends to increase the spatial extent of the region illuminated at the interface. The result a fundamental limitation on the attainable power density in contact with the switching interface and,

perhaps, to enforce a lower limit to the packing density of switching elements which can be attained.

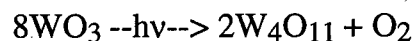
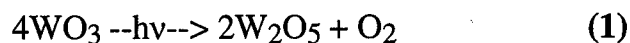
Various other hybrid approaches can be easily suggested depending on the electrochromic and photochromic properties of the active medium and the type of operation sought. To more fully illustrate the situation, we now turn our attention to the electrochromic and photochromic properties of the  $\text{WO}_3\text{-W}_2\text{O}_5$  system.

### The $\text{WO}_3\text{-W}_2\text{O}_5$ System

The electrochromic and photochromic properties of the  $\text{WO}_3\text{-W}_2\text{O}_5$  system have been well known<sup>7</sup> for over 30 years.  $\text{WO}_3$  is a yellow material which is a nominal semiconductor and represents the lowest energy form of tungsten in contact with molecular gas phase oxygen. It exists as a monoclinic solid<sup>8</sup> from room temperature to approximately 300° - 400°C. A first order phase transition to an orthorhombic form occurs in this temperature range, and very little evaporation of tungsten in any form occurs below 800° - 900° C.

Exchange of oxygen both within the lattice and between the solid and surrounding gas phase is well known<sup>9</sup>. The surface region of the material can be manipulated<sup>1</sup> so that it is more or less oxygen deficient with respect to stoichiometric  $\text{WO}_3$ . Oxygen deficiency leads to  $\text{W}^{+5}$  centers and the changing of the color of the material from yellow to blue. Concurrent with the color change, electrical properties, e.g. the electrical resistance, change by orders of magnitude<sup>3</sup>.

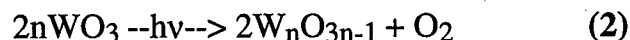
The change in the color in the  $\text{WO}_3$ - $\text{W}_2\text{O}_5$  system is indicative of a change in index of refraction which can be the basis for NIOS design. This change can be purely photochromic or electrochromic, or, as we have recently shown<sup>3</sup>, *simultaneously* driven by both electrical and optical stimulation. We summarized the purely photochromic approach using the following equations to emphasize the fact that the degree of oxygen deficiency



.

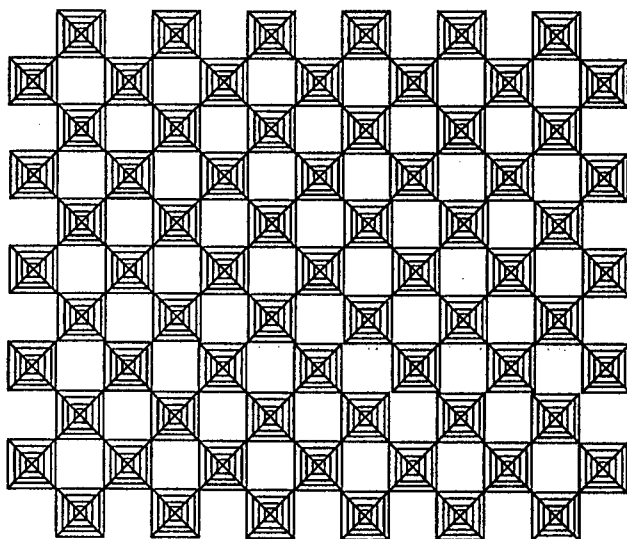
.

.

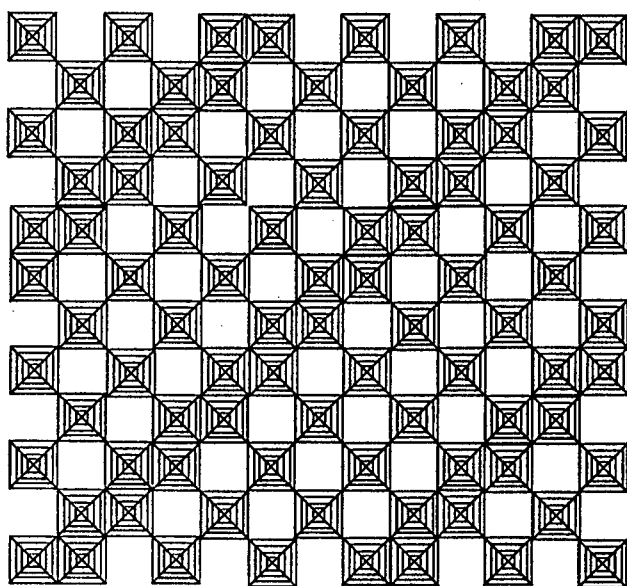


is highly variable and that an infinite number of modifications exist. These different forms, having general formula  $\text{W}_n\text{O}_{3n-1}$  are referred to as Magneli phases<sup>10</sup> and the coalescence growth<sup>11</sup> of these species on the surface of  $\text{WO}_3$  form what are known as "crystallographic shear" (CS) planes.

In the photochromic context, incident light is absorbed by the medium causing the formation of mobile oxygen atom and oxygen ion type species, which react with each other to form molecular oxygen. In the process, the  $\text{W}^{+6}$  on the  $\text{WO}_3$  is reduced to  $\text{W}^{+5}$  forming  $\text{W}_2\text{O}_5$ ,  $\text{W}_4\text{O}_{11}$  or higher order species of the form  $\text{W}_n\text{O}_{3n-1}$ . This molecular oxygen desorbs from the surface, thereby stabilizing the  $\text{W}_n\text{O}_{3n-1}$ . When the partial pressure of oxygen in the surrounding gas phase is sufficiently low, the equilibrium is



Idealized projection of the  $\text{WO}_3$  lattice. The concentric squares represent top views of  $\text{WO}_6$  octahedra. Note that all octahedra are corner sharing.



Idealized projection of crystallographic shear planes(113) showing edge sharing octahedra

Figure 3. Representation of packing of  $\text{WO}_6$  octahedra into lattice having either no edge-sharing octahedra, i.e.  $\text{WO}_3$ (top), or having edge-sharing octahedra,  $\text{WO}_{3-x}$ .

shifted towards  $W_nO_{3n-1}$  driven mostly by the large entropy increase due formation of gas phase oxygen from bound oxygen.

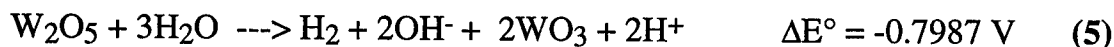
Concurrent with the loss of oxygen, the lattice rearranges from the corner sharing  $WO_6$  octahedra comprising the  $WO_3$  material to the rows of edge sharing octahedra comprising the  $W_nO_{3n-1}$ , the blue, reduced oxide. The arrangement of the octahedra determines the size and shape of the spaces, often long channels, in between the octahedra through which various species, including water, protons, and hydroxyl groups diffuse. Thus, the degree of oxygen deficiency determines the mobility of the reactants and products of the electronic and photochromic reactions.

For technologically interesting surfaces, adsorbed water and oxygen must be considered as being present. According to Yoshiike<sup>12</sup>, the presence of a proton donor enhances the photochromic response. In addition, the electrochromic response will certainly be enhanced by the presence of electrolyte, particularly if it is present in the channels. One way of representing the reaction is given below in Equations 3, 4, and 5.

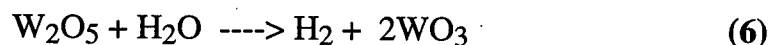
The water which is present on the surface and near surface regions of the oxide material is in equilibrium with ambient gas phase, i.e. air, and reacts under the influence of the appropriate applied potential gradient according to the following half-cell reactions<sup>2</sup>. There may be other reactions as well, although these reactions have been implicated by comparison with reactions thought<sup>13</sup> to occur on titanium oxide surfaces within the gas column spanning a scanning tip probe and the surface. The voltages are electrochemical potentials with the usual thermodynamic implications.



These comprise the net reaction summarized by reaction 5



which, if mass transfer allows mutual neutralization of  $\text{H}^+$  and  $\text{OH}^-$ , may be more accurately depicted as 6. The effects of mass transfer must be important to determining the lifetime of a written spot although the negative -0.7987 V electrode potential implies that the equilibrium position of 6 is far to the left, i.e. a "written" blue spot does not turn yellow spontaneously by reaction with ambient water.



It also seems probable that any  $\text{H}_2$  generated by 6 and  $\text{O}_2$  that is produced by 1, as well as atmospheric oxygen, combine to reform at least some of the  $\text{H}_2\text{O}$  making the overall process reversible to some extent. In some embodiments it will be useful to deposit the  $\text{WO}_{3-x}$  based layers on a conductive substrate, and when that is the case, it may be advantageous to use transparent platinum films such as are described by Chaiken<sup>14</sup>. In addition to having favorable electrical properties, it is thought<sup>15</sup> the platinum can catalyze the reaction to increase the speed of the electrochromic response for  $\text{WO}_{3-x}$  based materials.

It is clear that these reactions can also produce the molecular gases  $O_2$  and  $H_2$ , and that the reverse of the reactions can regenerate water at the expense of these gases whenever they accumulate within the lattice channels. Once the gases escape into the surrounding gas phase, or possibly even onto the exposed surfaces of the oxide, the reverse reaction becomes kinetically very slow. So-called "oxygen spillover" phenomena<sup>16</sup> involving surface diffusion of adsorbed oxygen from surrounding regions becomes important. A complex equilibrium should be expected involving chemical species which are common to both the electrochemical and photochemical processes. The combined action of the two processes might tend to maintain or degrade the reversibility of the medium.

The position of the electrochemical equilibrium with respect to changing temperature is not yet understood. Rapid heating and cooling can be achieved using infrared excitation. In addition to shifting the equilibrium, water and whatever other mobile phases are present can be expected to move out of the heated area. This motion can be along surfaces and grain boundaries or it could be in the channels through the lattice produced by the arrangement of the corner and edge sharing octahedra. On this basis we might expect to observe a shift in the real part of the index of refraction to smaller values leading to switching of the NIOS device composed of this medium. However we do not know yet whether the density of the filled solid phase changes to compensate for the loss of material in the channels. If it does, there could be no net change in the index.



Application of shorter wavelength light generates mobile oxygen vacancies which are also expected to change the index of refraction although in ways which might be difficult to anticipate. Based on the simple Drude model<sup>17</sup>, the increase in free charge density could lead to an increase in the index through a shift of the plasma frequency. Deposition conditions determine the degree of oxygen deficiency at the outset. The increased mass of the oxygen vacancies would be expected to affect the frequency response of the index.

Similarly, the process of applying a potential across a film should have the effect of injecting charge carriers into the lattice. Some of these will be trapped by  $W^{+6}$  centers to form  $W^{+5}$  centers, which we guess would tend to have the same effect as if the material were less oxygen deficient. This would also be expected to lead to an increase in the apparent index.

Depending on the water content, the effective applied potential and the initial degree of oxygen deficiency, there may or may not be a depletion region or other similar formation between the electrodes needed to impose the external electric field. Presently we will describe experimental methods before moving on to describe results. Since there are many issues relating to the basic operation of such devices, the purpose of this ES&E effort was to demonstrate the characteristics of NIOS devices based on the photo and electrochromism of  $WO_3$ .

## Experimental

Various films of the nominal formula  $WO_{3-x}$  were deposited on quartz disks, ZnSe disks, glass prisms, and ZnSe prisms. Films spanning a range of

thickness' spanning  $10^2$ - $10^3$  nm were deposited using a sputtering technique which we have been described elsewhere. In a future effort, it would definitely be useful to produce some devices using hydrogen during the deposition process. Presently, we produced films using only oxygen, argon and the tungstate target. These films have proton donors adsorbed to the surfaces and incorporated into the substrate before and during deposition.

Optical microscopy shows that these films are contiguous and very smooth. Imperfections on the films' surface appear to be caused by dust and other debris which is present during deposition or which collects afterwards. Thickness' were measured using a stylus profilimeter and the vertical excursions (z) for these films were actually only on the order of  $\pm 10^0$ - $10^1$  nm over a horizontal range (x,y) of millimeters.

UV-visible transmission spectra of these films were obtained using Shimadzu spectrometer and were identical to representative versions. IR reflectance spectra of these films, measured using a Harrick Seagull attachment on a Midac FT-IR spectrometer, are characteristic<sup>18</sup> of  $\text{WO}_3$  and  $\text{WO}_{3-x}$  films. Raman spectra were obtained using one of two different apparati. In the Syracuse University instrument, an  $\text{Ar}^+$  laser at 488 nm is used to excite scattering and in the Rome Lab instrument, either doubled YAG at 532 nm or  $\text{Ar}^+$  at 488 nm is employed. These apparati have been described in detail elsewhere<sup>3</sup>.

Electrodes were 100  $\mu\text{m}$  gold wires attached to the films using silver epoxy. Yellow  $\text{WO}_3$  films were colorized by placing a small, e.g.  $\approx 200 \mu\text{m} \times$

$\approx 200\text{ }\mu\text{m}$  x  $\approx 100\mu\text{m}$  thick piece of Sn or In foil in contact with the film and a few drops of 1 M HCl electrolyte<sup>6</sup>. Allowing the metal to be in contact with the electrolyte and the film for several minutes completely colorizes the initially colorless to yellow films to a dark blue. A longer treatment was not necessary but was often used. Once blue, the films could be washed and dried with a Kimwipe without changing the color or the texture of the film. When a potential was later applied to the films, a Keithley constant voltage source was used to maintain the bias.

A variety of optical setups were employed as shown on the next page. Figure 4 shows one approach used to measure Brewster's angle for some of the films on prisms. Although it would be trivial to automate this type of measurement, we only needed a couple representative curves to anticipate the angular dependence of the coupling of light into the films. Another approach is represented in Figure 5 which shows how "control" and "data" signals were combined and how the power of input and output light was sampled.

## Results

Most of the previous work utilizing the POMS process has involved using fully oxygenated  $\text{WO}_3$  samples which are yellow, comparatively insulating and possess a strong Raman spectrum. Most of the work done in this effort involved using blue oxygen-deficient films,  $\text{WO}_{3-x}$ . These blue films absorb incident light much more strongly and therefore are easier to manipulate photochemically. They correspond to the "written state" of the POMS process as it was originally presented. These films are much better

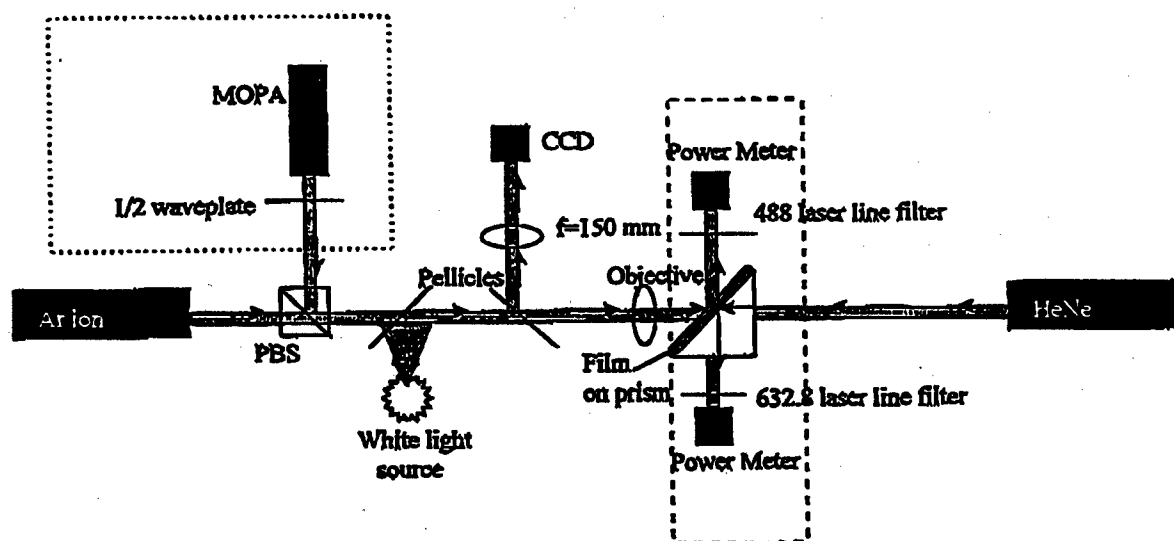


Figure 4. Optical set-up for probing prism type NIOS configurations.

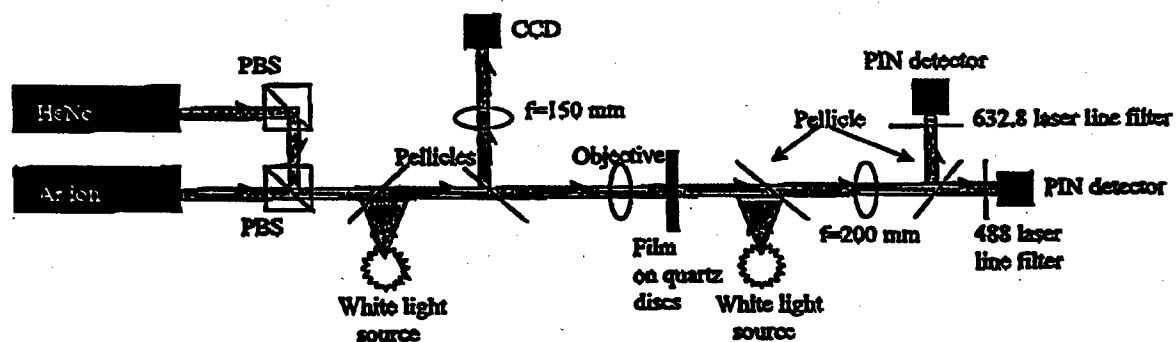


Figure 5. Optical set-up for probing  $\text{WO}_3$  films on planar substrates.

electrical conductors and the blue material has essentially no Raman features. The lack of conductivity of the yellow films precludes much direct charge injection although our earlier work has shown that photostimulation is electrically detectable.

Regarding the yellow film's optical response to electrical stimulation, we have the well known electrochromism. Thus, the result of that electrochromism, the formation of the blue films, was employed in this work. Careful metalization could allow incorporation of the electrochemical processes into the basic NIOS device structure.

Our results show that as-deposited blue films, and yellow films which have been turned blue electrochemically, behave essentially identically with regard to the laser processing employed in this study. This is in spite of the fact that the electrochemically treated films have positive ions of Sn and In injected into the  $\text{WO}_3$  lattice. This is important because it means that devices which start with a blue film and produce a yellow film photochemically in the process of storing or switching data, can be *erased or reversed* electrochemically.

A typical angular response of the switches is represented by the curve in Figure 6. The reflected  $\text{Ar}^+$  or HeNe power was measured as a function of angle of incidence with the goal to characterize the interface between the prism and the active film. This would allow us to determine the index of refraction of the film and precisely state the degree of evanescent wave propagation at the interface. This occurs, of course, at the minimum of the reflectance versus angle curve. We shall return to this issue later. These

results are similar to those of Ledeider<sup>19</sup>. The power levels used to obtain these spectra were varied and, given the results we shall present below, some of the variability is probably due to photorefractive response of the films.

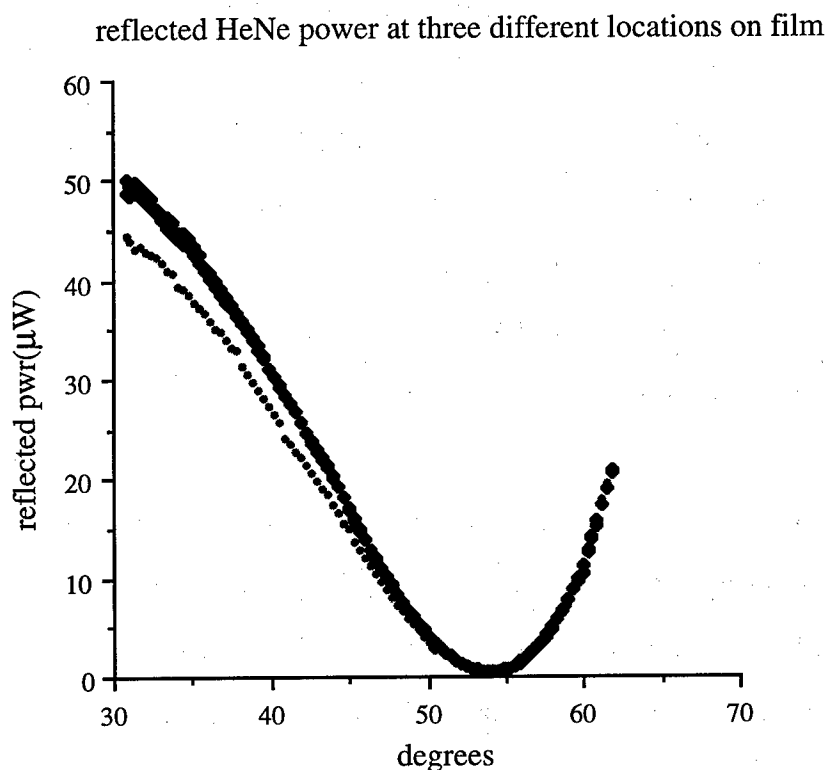


Figure 6. Angular response on three different positions on blue film.

Sets of switches were fabricated at the CNF in which the substrate was varied between being glass( $n=1.6$ ) and ZnSe( $n=2.6$ ) and the films were either high oxygen content, nominally yellow, with  $n \approx 2.2$ , or they were low oxygen content, quite blue with  $n \approx 2.4$ . ZnSe was chosen to contrast the glass as substrate because its index of refraction is much closer to that of the active film than is either glass or quartz. The effect of the substrate-film interface will therefore be different for the two choices of substrate.

Using the apparatus of Figure 4, each of these switches was tested using the following procedure. The  $\text{Ar}^+$  ion power was ramped upwards in steps, and the power of the HeNe which is transmitted through the prism is measured. The HeNe angle of incidence was chosen to be  $53.878^\circ$  so that trials were conducted for which it was initially on the low side of Brewster's angle. In these ramping experiments, care was taken to move through the measurements in a methodical and even pace. Since there is the possibility that some of the films' photorefractive response is due to the accumulated exposure to light, relatively constant time intervals between measurements leads to semiquantitative knowledge of the accumulated dose of control light.

As can be seen in a typical case depicted in Figure 7, for sufficiently small spot size, there is always a power which when applied, leads directly to a discontinuous change in the transmission and reflectivity sensed at the film. Trial and error showed that the amount of change, that is, the percentage change in the sensed power of either the HeNe or the  $\text{Ar}$  ion light, depends critically on the spatial overlap between the control and the data beams. In the present case the  $\text{Ar}^+$  ion light was the control and the HeNe light was considered the data.

Once the discontinuous change occurs, another effect was always observed. There was a much smaller amplitude modulation in the HeNe reflectivity induced by modulating the  $\text{Ar}^+$  beam. This modulation was never much more than  $\approx 15\text{-}20\%$  and eventually, after thousands of cycles, this modulation became smaller in amplitude.

Discontinuous variation in HeNe power with increasing 488 nm excitation

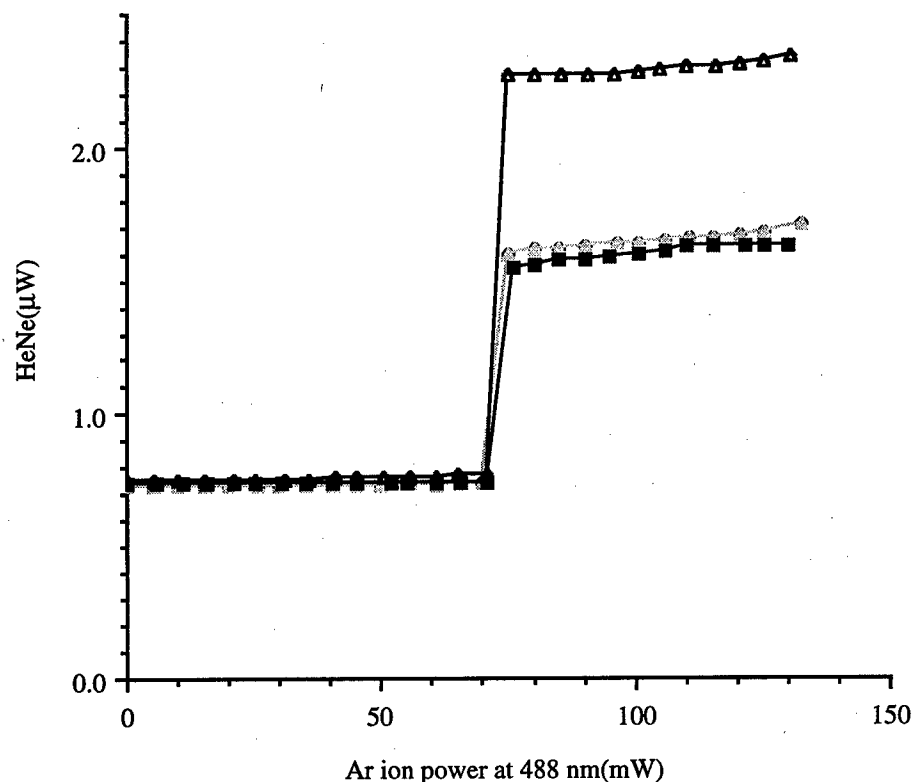


Figure 7. "Ramp" experiment showing threshold for switching.

This overall behavior is illustrated by the oscilloscope trace shown in Figure 8. In this case, the laser power was  $\approx 40$  mW and the spot size was  $\approx 15 \mu\text{ m}$ . On first exposure to the  $\text{Ar}^+$  light, the reflectivity of the HeNe changed drastically. Subsequent modulation of the  $\text{Ar}^+$  beam resulted in distinct modulation of the HeNe reflectivity but the modulation was much less than the initial modulation concurrent with "writing" the observable spot. Note that the rise time of the shuttered  $\text{Ar}^+$  control beam was  $\approx 60 \mu\text{sec}$  and that the response on the HeNe switching, after the first large modulation, was always about a factor of 2-5 times slower regardless of



the laser power. The first large modulation was much faster, approaching the time profile of the control light.

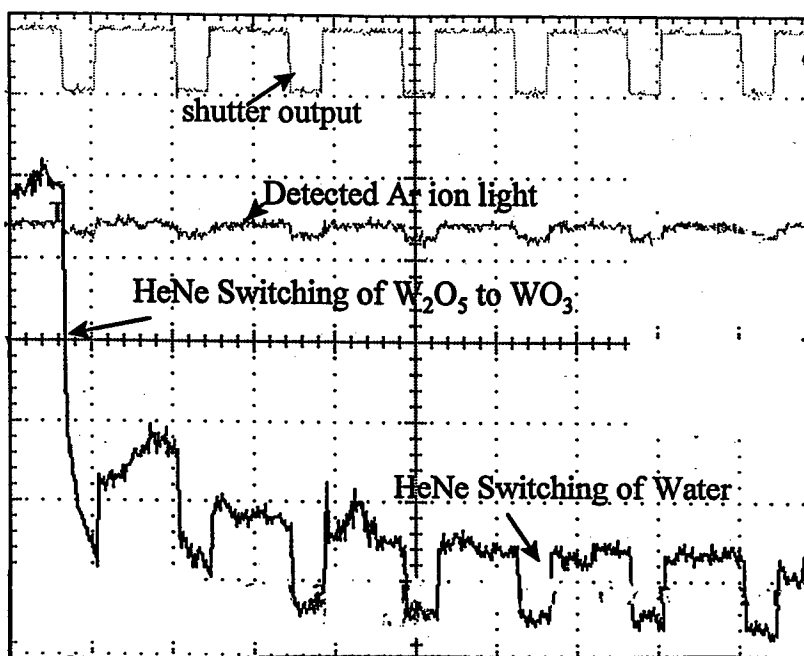


Figure 8. Oscilloscope trace showing two regimes of switching.

In another experiment, the Raman spectrum of the blue films was taken at different applied powers of the Ar<sup>+</sup> light. At some point, in a similar discontinuous fashion, the Raman spectrum changes from having no features below 1000 cm<sup>-1</sup> to having the full spectrum of the yellow material including the 802 cm<sup>-1</sup>, 716 cm<sup>-1</sup>, features and the clump of lines near 200 cm<sup>-1</sup>. Thus the material assumes the corner sharing octahedra motif when the discontinuous change occurs.

In addition to the change in the Raman spectrum, the change in refractive index results in different reflectance and transmission characteristics. These are clearly shown in Figure 9. The blue films, when backlit with white light, transmit very little light. The field of view is therefore dark blue. After being, "written", i.e. the Raman changes and the discontinuous refractive index change occurs, a spot can be seen in the films. When backlit, the small spot appears with essentially the same color as the illumination lamp light.

We have "written" such "bleached" spots with very little light and, depending on the focusing objective used, spots as small as  $1.5\text{ }\mu\text{m}$  in diameter have been produced. It is clear that with more effort smaller spots are possible. Depending on the laser power levels employed and the duration of the exposure, a variety of written features can be observed. Close examination of all written spots reveals that they usually have well defined edges and that, when the diameter is sufficiently small, there is often a dark spot in the middle. Around the outside edges of spots written with high power or longer duration exposure, there is a "depletion zone" which is lighter than the surrounding blue material but not identical in appearance to the inside the spot. When the spots are small, there is a clear set of diffraction rings on the transmitted HeNe light beam. Profilimetry failed to show laser induced surface topography changes, so all indications are that the appearances are due to changes in the optical properties of the material and not due to changes correlated with surface roughness.

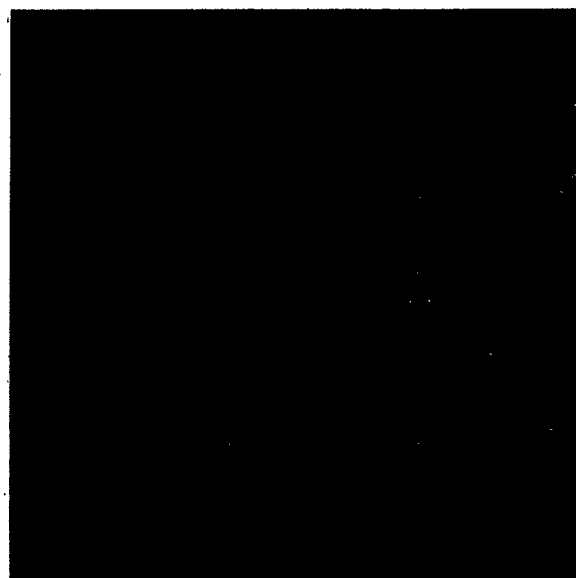
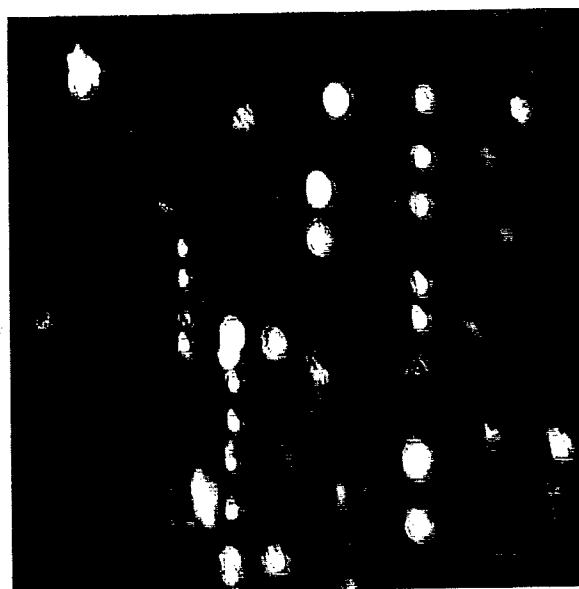
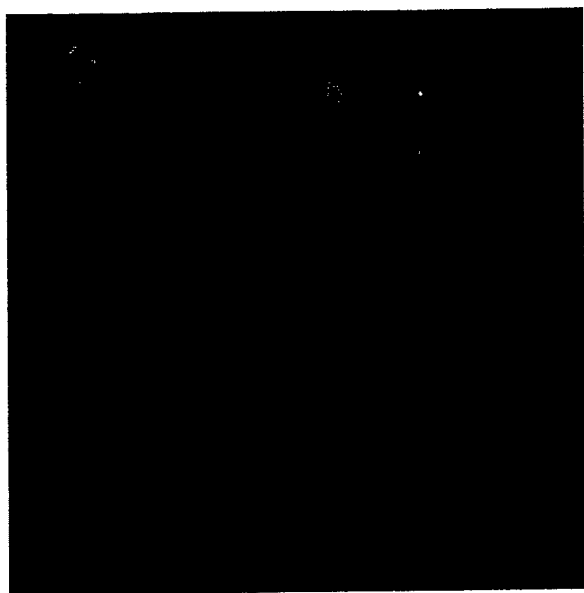


Figure 9.

Appearance of "written" spots on blue film using red(top), white(middle), and blue(bottom) backlighting.

These experiments all used either a single  $\text{Ar}^+$  ion beam, a single MOPA (985 nm) beam, or a combination of the two. As expected from all of our previous work on the POMS process, the principal effect of the MOPA beam was to lower the writing threshold for the  $\text{Ar}^+$  beam. The thresholds for writing with either beam alone is greater than that for the simultaneous use of both beams.

Two types of experiments were conducted which are revealing with respect to the dual-mode potential of these NIOS based devices. The results obtained using films which were produced blue by the sputtering process were reproduced using films which were produced yellow by the sputtering process but which were first colored electrochromically. Indeed, the ramp experiment shown in Figure 7 shows that the discontinuous change occurred in much the same way whether the films were produced blue by the sputtering process or whether they were electrochemically colored. This experiment mimics the response expected for a switch based on Figure 2b.

The last type of measurement was on a device based on Figure 2a. In this case a potential was applied across two electrodes while the laser excitation was applied between the electrodes. The configuration in which the applied static electric field is perpendicular to the film surface was not attempted in this effort. These trials also demonstrated very similar results to those for the purely optical versions. The electric field had some effect on the switching of these devices, but it is not very dramatic compared to the effect of the applied laser light.

In an attempt to extrapolate the response of the films to higher power, short time duration light pulses, another set of measurements was conducted. In these experiments, the net response of the films was measured as the power and duration of the exposure was changed in a concerted fashion. These results allowed us to observe the degree to which the net response was a function of the amount of energy deposited into the sample as opposed to the peak power or the net time duration. As

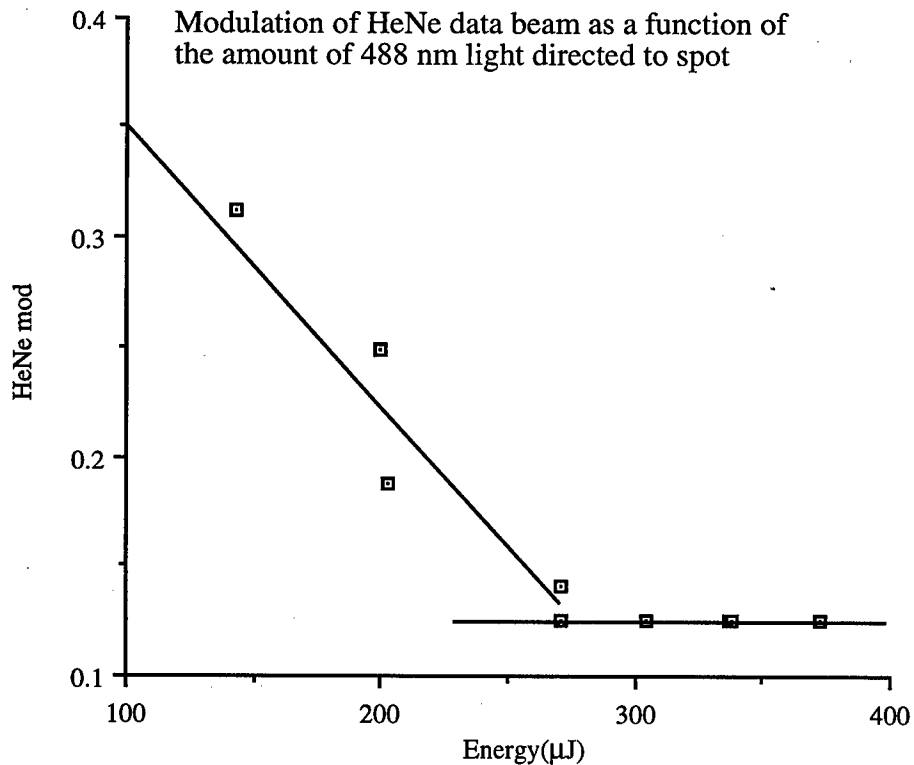


Figure 10. HeNe modulation as a function of applied 488 nm energy.

can be seen from the graph in Figure 10, the total energy exposure does correlate roughly linearly with the degree of HeNe modulation, i.e. the net change in detected reflected power.

## Discussion

We believe the results of this effort are quite impressive. For the first time, all optical, fully reversible, switch operation based on the NIOS structure and the POMS process was clearly demonstrated. This switching occurs in two regimes. The first, clearly revealed by the change in the Raman spectrum and the discontinuous change in the index of refraction, involves the formation of corner sharing octahedra from the amorphous collection of structures produced during the sputtering process. This process is mostly irreversible under the conditions of these experiments. The second regime is quite reversible and is represented by the much lower amplitude index of refraction modulation which occurs after the first discontinuous change. We shall discuss each regime separately.

In the first discontinuous change, the material is being changed from  $W_2O_5$  (and its higher analogues) to  $WO_3$  and its corner sharing octahedral internal microscopic structure. This is evident by the variation in the Raman spectra and the other optical properties. This change can be "erased" by electrochemical treatment. The results clearly show that electrochemically colored material can be written on in exactly the same way as sputtered blue films. Therefore, this study has shown that blue films can be written photochromically and erased electrochromically. The temporal response of the erase process for these films is expected to be

slow, presently millisecond timescale, but erase speed is often not as important as write speed.

Speed of reaction would seem also to be the most important difference between the electrochromic process and the photochromic process. The relative insensitivity of the photodriven switching response to application of an external electric field suggests that the electrochromic reaction is much slower than the photochromic reaction. Apparently the motion of injected charge, or possibly the reaction products produced by charge injection, is too restricted or intrinsically slow to compete with that associated with photoexcitation. In either case, presently it seems unlikely that electrochemical bias can be used to increase the switching speed of devices based on the  $\text{WO}_3\text{-W}_n\text{O}_{3n-1}$  system.

On the other hand, because of the observed correlation between the net change in film index of refraction and the amount of energy exposed to the film, the photochromic write speed, particularly in the blue to yellow direction, is expected to be quite fast. Based on the results, the known thermodynamics of the  $\text{WO}_3\text{-W}_n\text{O}_{3n-1}$  system, and the availability of higher power lasers which can be modulated at very high speeds, one can envision achieving 10-50 nsec write times. In the present work, lower power, CW lasers were employed and so if there are any power dependant processes which also can occur, the above estimate could be either too fast or even too slow. For example, Yoshiike has reported switching times for the slower yellow to blue transition of 200 psec.

The second regime of switch which was observed is extremely interesting due to its resilience and reversibility. First, it is clear that water plays a central role in the chemistry of the electro and photochromism of the  $\text{WO}_3\text{-W}_n\text{O}_{3n-1}$  system. It is also well known that water can be trapped in and move throughout the lattice of  $\text{WO}_3\text{-W}_n\text{O}_{3n-1}$  type systems. Water adsorption has been shown to be easily observed using Brewster Angle Microscopy. This type of microscopy is, in actual fact, identical to NIOS operation. Adsorption of even pure water on the otherwise uncoated hypotenuse of a prism forms a layer which acts in a fashion analogous to the  $\text{WO}_3\text{-W}_n\text{O}_{3n-1}$  system layer employed in these experiments.

The clear region surrounding the written spots demonstrates that it is possible to induce the yellow to blue transition without necessarily inducing a large breakdown in the lattice. It seems probable, although it is not yet certain, that within this regime, the observed reversible modulation becomes possible. Note that the applied infrared light and the blue light have nearly the same effect. So, since the infrared light probably does not have sufficient energy per photon to directly excite the motion of charge carriers, one effect of both forms of excitation is to heat the lattice and drive the motion of water in the lattice.

There has been considerable controversy in the literature concerning the degree to which the well known photo and electrochromic behavior of these materials involves water or oxygen loss. We believe our results support the notion that the first big effect involves the loss of oxygen whereas the reversible modulation involves some effect which does not change either the color or the Raman spectrum of the spots. The speed of



these switches is relatively slow,  $10^2$   $\mu$ sec for either turn on or turn off. All of these observation show that the reversible effect involves more water mediated chemistry or some type of physical effects.

While there can be little doubt that much has been learned about the use of  $\text{WO}_{3-x}$  based systems for optical switching, much remains to be learned to fully exploit the possibilities we have discovered. Faster timescale measurements and attempts to study devices incorporating water or hydrogen in other forms in a more controlled manor are indicated.

### Conclusions

It is possible to produce complete reversible all optical switching of visible light using sputtered  $\text{WO}_x$  films. The effects are so robust that while a NIOS structure can be used and may be advantageous for some purposes, it is not absolutely necessary to produce such switches. These devices can operate like a latching flip-flop or in other ways depending on the need.

### References

---

1. R. M. Villarica, Fazio Nash, J. Chaiken, J. Osman, R. Bussjager, Proc. Mat. Res. Soc. **397**, 347(1996)
2. R. Bussjager, J. M. Osman, M. J. Cote, J. Chaiken. J. Appl. Phys., submitted
3. R. Bussjager, J. M. Osman, J. Chaiken, Proc. SPIE, **3075**, 34-46(1997)
- \* 4. J. Chaiken, Final Technical Report RL-TR-94-238

\*RL-TR-94-238 is limited to US Government agencies only.

- 
5. Peter W. Smith, W. J. Tomlinson, Patrick J. Maloney, J. P. Hermann  
IEEE J. Quant. Elec., **QE-17**, 340(1981)
  6. Richard S. Crandall and Brian W. Faughnan; Appl. Phys. Lett, **26**,  
120121(1975) and numerous others therein
  7. S. K. Deb, Appl. Opt. 801(1972)
  8. A. Hamnett and J. B. Goodenough, in "Semiconductors," Ed. O.  
Madelung, Landolt-Bornstein Numerical Data and Functional Relationships  
in Science and Technology. New Series, Group III, Volume 17g, Part III  
(Springer, Berlin, 1984)
  9. E. R. S. Winter, J. Chem. Soc. A., pp. 2889-2902(1968)
  10. M. Sundberg and R. J. D. Tilley, J. Solid State Chem. **11**, 150-  
160(1974)
  11. F. H. Jones, R. A. Dixon, A. Brown, Surf. Sci. **396**, 343-350(1996)
  12. Yoshiike, US Patent 4,711, 815
  13. H. Sugimura, T. Uchida, N. Kitamura, H. Masuhara J. Phys. Chem. **98**,  
4352-4357(1994)
  14. Chaiken, US Patent 4,971,853
  15. I. F. Chang, IBM Technical Disclosure Bulletin **19**, 326-327(1976)
  16. G. Mestli, P. Ruiz, B. Delmon, H. Knowzinger J. Phys. Chem. **98**, 11269-  
11275(1994)
  17. for a good review see Henry Ehrenreich, IEEE Spectrum, March 1965,  
pp. 162-170
  18. M. F. Daniel, B. Desbat, J. C. Lassegues J. Solid State Chem. **73**, 127-  
139(1988), J. Solid State Chem. **67**, 235-247(1987)
  19. C. Bechinger, E. Wirth, P. Leiderer Appl. Phys. Lett. **86**, 2834-  
2836(1996)